

Reflow Microfabrication for Refractive Optical Components: Processes and Materials

R.W. Johnstone and M. Parameswaran

Institute for Micromachine and Microfabrication Research, School of Engineering Science
Simon Fraser University, 8888 University Dr., Burnaby, BC, Canada, V5A 1S6

ABSTRACT

With standard surface-micromachining, free-space micro-optical-benches can be constructed that contain mirrors and diffractive optics. This paper outlines a novel microfabrication process for integrating refractive optical elements, such as lenses, into surface-micromachining processes. The process involves melting the optical material after the raised structures have been assembled. The resulting lenses can have a wider range of focal lengths, and can be made from a wider variety of materials than previous work. This technique will allow integration and customization of micro-optical and micro-photonic systems for various application.

Keywords: reflow fabrication, micro-optics, refractive lenses, surface-micromachining

1 INTRODUCTION

The seminal paper on the topic of free-space micro-optical systems was written by Pister *et al* [1], which demonstrated several optical components that were fabricated using surface-micromachining [2], [3]. Surface-micromachining is a planar fabrication process, and excels at constructing integrated mechanical systems in the two dimensions parallel to the wafer surface. However, surface-micromachining does suffer an important disadvantage in that far less control is available in the third dimension. Further, the total available height is usually limited to less than $10\mu\text{m}$.

The paper by Pister *et al* introduced surface-micromachined hinges, allowing the construction of fully 3D structures. With hinges, components are fabricated flat and then raised to a standing position after release [1]. Geometric control during processing is still only in the two dimensions parallel to the wafer surface, and surface-micromachining is still only capable of constructing flat structures. However, these flat structures can be oriented in new positions during the assembly process.

The literature not only discusses various types of surface-micromachined hinges, but also demonstrates several novel surface-micromachined structures, including several optical components. In particu-

lar, the method has been used to construct surface-micromachined mirrors and diffractive optics [4]–[9].

The main difficulty with the optical components available to date is the lack of refractive optical components, particularly lenses. While diffractive elements, such as Fresnel-zone plates, can approximate refractive lenses, they only work at a single wavelength and suffer high optical losses [5], [10]. Even with novel materials, standard surface-micromachining techniques cannot be used to construct refractive components because they contain no provisions for curved surfaces. Therefore, we are investigating a new method of microfabrication that will allow us to fabricate miniature refractive components.

Integrated refractive components have been reported. King *et al* [10] demonstrated a refractive lens fabricated using photoresist, but significant improvements can be made. The process we are developing, outlined below, will be capable of a greater range of $F\#$'s and will use better optical materials.

2 FABRICATION PROCESS

Reflow microfabrication is a modification of standard surface-micromachining techniques [2], [3], and does not limit the construction of structures available using conventional surface-micromachining. In our proposed fabrication process, the wafers undergo a complete surface-micromachining process with at least two moveable structural layers, such as PolyMUMPsTM. An additional structural layer, called the 'reflow' layer, is then deposited upon the wafer and patterned, before the release step. Because this layer is composed of the material that will be used to construct the refractive components, and so it should be a suitable optical material. Additionally, the material for the 'reflow' layer is chosen to have a melting point below that of the other structural materials in the surface-micromachining process. Processing then continues with the removal of the sacrificial material [2], [3] and the assembly of the 3D structures [1].

The entire system, containing the assembled structures, is then heated until the 'reflow' material melts. Surface tension pulls the 'reflow' material into droplets (figure 2). For miniature devices, gravity plays a negli-

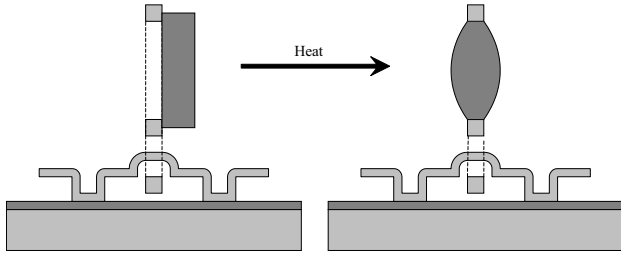


Figure 1: Illustration reflow fabrication process for forming refractive lenses.

gible role in determining the final shape of the droplets. The droplets' shapes are thus determined by surface tension, and so the liquid-air interfaces should be spherical. Therefore, carefully constructed droplets can be used to construct refractive components.

The key difference between this process and the process outlined by King *et al* [10] is the timing of the reflow. By performing the reflow after assembly, lenses can be formed with two spherical surfaces instead of one. The additional spherical surface allows for lenses with much smaller focal lengths.

3 THEORY

3.1 Focal length and droplet volume

The focal length of a thin lens can be determined from the radii of curvature of the lens' two surfaces [11].

$$\frac{1}{f} = \frac{n_2 - n_1}{n_1} \left(\frac{1}{R_1} + \frac{1}{R_2} \right) \quad (1)$$

In equation 1, f is the focal length, n_1 is the index refraction of the ambient material (air), n_2 is the index of refraction of the lens material, and R_1 and R_2 are the radii of curvature for the lens's two surfaces.

However, since the pressure difference between the atmosphere and the droplet will be constant at equilibrium, it follows from the Laplace-Young equation [12] that the two radii of curvature must also be equal. Equation 1 can then be rearranged into the following equation:

$$R = 2 \frac{n_2 - n_1}{n_1} f \quad (2)$$

One would now like to determine the droplet's total volume. However, a more careful look at the droplet's contact angle is necessary before one can calculate the droplet's volume. The contact angle is a material property, and is fixed independent of fluid volume or radius of curvature. On a flat surface, the radius of curvature and the contact angle would fix the diameter of

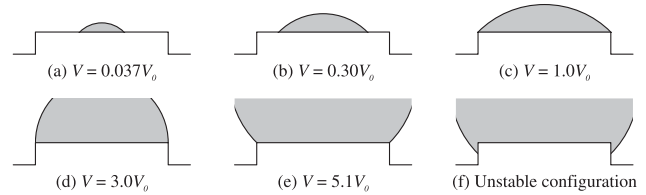


Figure 2: Illustration of heat treatment in reflow fabrication process

the lens. However, the aperture diameter and the focal length are central to lens design, so a way to vary the contact angle is necessary. One can vary the effective contact angle by changing the local slope of the surface. This is most easily accomplished by using a raised platform (figure 3.1). Although drawn as a sharp corner, a fillet, although microscopic, exists at the corner. This allows the effective radius of curvature to vary, even if the real contact angle is fixed.

$$\theta^* \in [\theta, \theta + \pi] \quad (3)$$

Above, θ^* is the effective contact angle, and θ is the real contact angle. This concept can be extended to reflow lenses, which are supported by a circular annulus (figure 2). Note that in this case, there are two corners, an inside and an outside, at which the effective contact angle can vary. With both inside and outside corners, the effective contact angle can vary between $\theta - \pi$ and $\theta + \pi$.

Assuming that the droplet is attached to the inside corner of the supporting annulus, the total droplet volume can be calculated using the following formula. In the opposite case, where the droplet is attached to the outside corner, the following formula is still used, but the volume of the annulus is subtracted from the result.

$$V = t\pi r^2 + 2 \int_{R_0}^R \pi (R^2 - r^2) dr \quad (4)$$

$$V = t\pi r^2 + \frac{4}{3}\pi R^3 + \frac{2}{3}\pi R_0^3 - 2\pi R^2 R_0 \quad (5)$$

In equation 4, the first term represents the cylindrical volume defined by the interior of the annulus, and depends on the thickness of the annulus, t , and the inner radius. The second term accounts for the two spherical sections that make up the droplet's volume outside the annulus' inner space, and depends on the radius of curvature, R , and the distance from the centre of curvature to the spherical section, R_0 . This distance can be calculated by noting that the radius of curvature, the lens radius, and R_0 form a right-angle triangle. This results in the following equation for R_0 :

$$R_0 = \sqrt{R^2 - r^2} \quad (6)$$

Equation 6 imposes the condition that the radius of curvature must be greater than the lens' radius. Physically, this simply indicates that if the radius of curvature was too small, the droplet would not reach the supporting annulus. The condition $r < R$ can be combined with equations (1) and (2) to develop a lower limit on the $F\#$ of lenses, where $F\#$ is the ratio of the focal length to lens diameter.

$$F\# > \frac{n_1}{4(n_2 - n_1)} \quad (7)$$

Equation (7) indicates that materials with high indices of refraction make better lens materials since they allow for lenses with shorter focal lengths. However, this advantage must be traded against the higher reflective losses that will occur [11]. The lens material thus represents a trade-off.

As previously mentioned, the limits expressed by equation (7) are the result of manufacturing limits. These limits are also represented in the range of possible droplet volumes. To achieve the minimum possible focal length, one must have the largest allowed droplet size, which occurs when $R = r$, as discussed when deriving equation (7). Similarly, to achieve the largest possible focal length, one must have the smallest allowed droplet size, which occurs in the limit as $R \rightarrow \text{inf}$.

$$V_{\min} = t\pi r^2 \quad (8)$$

$$V_{\max} = t\pi r^2 + \frac{4}{3}\pi r^3 \quad (9)$$

The above two equations are important because they indicate the range of volumes a fabrication process must support in order to achieve the full range of focal lengths possible. The 'reflow' material will be patterned, so volume can be easily removed from the starting material, and hence from the resulting droplet. Assuming that all the material for the droplet will be deposited over the aperture of the lens, then equation (9) can thus be used to determine the necessary thin-film thickness necessary for the 'reflow' material.

$$h = \frac{V_{\max}}{\pi r^2} = t + \frac{4}{3}r \quad (10)$$

For equation 10, the thickness of the 'reflow' material, h , is a function of two terms. The first term will be constant for all lenses on a single chip, and so does not pose a problem. However, the second term depends on the lens' aperture, and this parameter can change from lens to lens. A particular process will therefore be optimal for a particular lens diameter; lenses with smaller apertures can be fabricated, but not larger apertures.

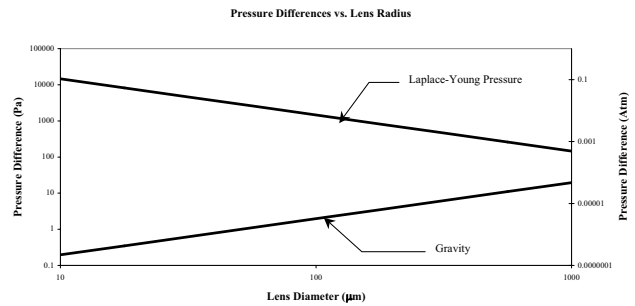


Figure 3: Plot of pressure differences caused by (a) curvature of the droplet surface, known as the Laplace-Young pressure, and (b) pressure gradient induced in the droplet by gravity. The droplets were of water.

3.2 Lens shaping by surface tension and gravity

In the previous section, the effect of gravity on the lenses' shapes was neglected. For surface-tension to dominate the shape of the lens, pressure changes in the body of the droplet due to gravity must be negligible. Both of these pressures are easily calculated for droplets of various sizes (figure 3.2).

By comparing the pressure differences due to the Laplace-Young equation [12] and gravity, a limit on droplet sizes can be obtained. We introduce a dimensionless number that relates the importance of surface tension and gravity in determining a droplet's shape:

$$\eta \equiv \frac{\rho g r R}{\sigma} \quad (11)$$

Above, η is the ratio of the Laplace-Young and gravity pressure differences, which depends on key note is r , the lens' aperture radius, and R , the lens' radius of curvature. Equation (14) represents a limit on the product of these two design variables.

The results in figure 3.2 were verified by performing a series of volume-of-fluid (VOF) analyses using ANSYSTM. In these simulations, the gravitational acceleration was varied between its true value of 9.81 ms^{-2} and $9.81 \times 10^5 \text{ ms}^{-2}$ for a lens with a radius of $10 \mu\text{m}$. Distortions of the lens' shape were not visibly noticeable until gravity had been increased by a factor of 10^5 , not the 10^4 as predicted by figure 3.2, although optically significant distortions did appear earlier.

4 MATERIALS

We are currently investigating both inorganic and organic materials for use as the reflow material in this process. We are currently focusing on poly(methyl methacrylate), or PMMA, as our organic material. A particular inorganic material has not yet been chosen, but we are planning to select a halogenated salt.

Most of our work to date has focused on PMMA. This thermoplastic is a common optical material, and is also known as Plexiglass. PMMA was chosen because it is a thermoplastic, and so can be melted and reformed. Further, PMMA exhibits a true melting point in addition to a glass transition temperature. This makes it a good candidate for reflow microfabrication.

While the PMMA does reflow, our efforts at fabrication have been hampered by the extremely high viscosity of PMMA. For example, the zero-shear viscosity of PMMA with a molecular weight of 10^5 is approximately 10^6 Pas at 190°C [14]. For comparison, the viscosity of water at room temperature is near 10^{-3} Pas. The reflow process thus takes a long time. The viscosity can be lowered by increasing the temperature, but oxidation and decomposition are a concern. Further work at higher temperatures is planned.

For inorganic reflow materials, we also plan to develop processes using halogenated salts. Many of these materials are commonly used as optical materials. We wish to keep the process as generic as possible, so that all of these materials may be used. This would offer a range of transmission windows and refractive indices.

Unfortunately, many of the halogenated salts are soluble in water. This complicates manufacturing, as the surface-micromachined chips will still need to be released after deposition and patterning of the reflow layer, and the solvent of common oxide etchants is water. However, the manufacturing process can compensate. Currently, we are considering two different methods of preventing damage if the halogenated salt is water soluble:

- It may be possible to pre-load the solutions with the appropriate ions. This would lead to a solution already at the solubility limit, and prevent etching of the reflow material. However, cross-solubility products with the desired etchants must be considered.
- The reflow material can be encapsulated during release. The simplest approach would be to use photoresist. While this limits solution interactions, it would require an additional mask step.

5 CONCLUSION

At micro-scale lengths, the shape of liquid droplets is influenced far more by surface tension than gravity. This fact can be used to construct refractive optics for miniature free-space optical systems. Lenses can be constructed using standard planar processing techniques and a simple post-process heat treatment.

The focal length of the fabricated lenses can be determined using the geometry of the supporting annulus and the droplet's volume. Designers could thus con-

trol both the aperture and focal length of the fabricated lenses.

REFERENCES

- [1] K.S.J. Pister, M.W. Judy, S.R. Burgett, and R.S. Fearing. "Microfabricated Hinges," *Sensors and Actuators A*. vol. 33, no. 3, pp. 249-256 (1992).
- [2] R.T. Howe. "Surface micromachining for microsensors and microactuators," *Journal of Vacuum Science and Technology B*. vol. 6, no. 6, pp. 1809-1813 (1988).
- [3] J.M. Bustillo, R.T. Howe, and R.S. Muller. "Surface micromachining for microelectromechanical systems," *Proceedings of the IEEE*. vol. 86, no. 8, pp. 1552-1574 (1998).
- [4] K.Y. Lau. "MEM's the word for optical beam manipulation," *IEEE Circuits and Devices*. vol. 13, no. 4, pp. 11-18 (1997).
- [5] M.C. Wu. "Micromachining for optical and optoelectronic systems," *Proceedings of the IEEE*. vol. 85, no. 11, pp. 1833-1856 (1997).
- [6] R.S. Muller and K.Y. Lau. "Surface-micromachined microoptical elements and systems," *Proceedings of the IEEE*. vol. 86, no. 8, pp. 1705-1720 (1998).
- [7] A. Friedberger and R.S. Muller. "Improved Surface-Micromachined Hinges for Fold-Out Structures," *Journal of Microelectromechanical Systems*. vol. 7, no. 3, pp. 315-319 (1998).
- [8] Y.W. Yi and C. Liu. "Assembly of micro-optical devices using magnetic actuation," *Sensors And Actuators A*. vol. 78, no. 2-3, pp. 205-211 (1999).
- [9] L. Zhou and J.M. Kahn. "Corner-Cube Retroreflectors Based on Structure-Assisted Assembly for Free-Space Optical Communication," *Journal of Microelectromechanical Systems*. vol. 12, no. 3, pp. 233-242 (2003).
- [10] C.R. King, L.Y. Lin, and M.C. Wu. "Out-of-plane refractive microlens fabricated by surface micromachining," *IEEE Photonics Technology Letters*. vol. 12, no 10, pp. 1349-1351 (1996).
- [11] F.L. Pedrotti and L.S. Pedrotti. *Introduction to Optics: Second Edition*. Prentice Hall, Englewood Cliffs, 1987.
- [12] C. Isenberg. *The Science of Soap Films and Soap Bubbles*. Dover Publications, New York, 1992.
- [13] G. Elert, Ed. *Density of Air*. [Online] Accessed: 2004/10/29. Available: <http://hypertextbook.com/facts/2000/RachelChu.shtml>
- [14] K. Fuchs, C. Friedrich, and J. Weese. "Viscoelastic Properties of Narrow-Distribution Poly(methyl methacrylates)," *Macromolecules*. vol. 29, no. 18, pp. 5893-5901 (1996).